Nonlinear luminescence of stacking-fault excitons in BiI_3 induced by the exciton-exciton Auger process

Tomobumi Mishina, Hiroaki Chida,* and Yasuaki Masumoto
Institute of Physics, University of Tsukuba, Tsukuba, Ibaraki 305, Japan
(Received 26 October 1992)

We have studied the optical nonlinearities of stacking-fault excitons in layered crystals of BiI_3 by means of luminescence spectroscopy. From a measurement of the excitation density dependence of the luminescence we find a saturation of the intensity and an increase in the decay rate. Especially at high excitation densities, the decay curve of the T exciton shows a clear nonexponential decay which is well fitted by a nonlinear differential equation. We have also observed the time correlation signal of the nonlinear luminescence. These experimental findings show that an Auger exciton-exciton annihilation process is dominant over that of optical nonlinearity of the stacking-fault excitons.

Recently the dynamics of photogenerated carriers and the resultant optical nonlinearities in semiconductor materials have attracted much attention from both the fundamental and applied points of view. For a study of the dynamics of the photogenerated carriers, time-resolved luminescence spectroscopy is a powerful tool, and provides information about carrier dynamics in semiconductor systems such as carrier cooling, spin relaxation, and recombination processes.[1-5] The Auger process is one of the interesting and important processes of semiconductor materials under high-excitation conditions. In highly doped semiconductors, the Auger process is considered the dominant nonradiative process,[6,7] and, in Cu_2O, an Auger exciton-exciton annihilation process is discussed as the quantum saturation mechanism at the phase boundary for Bose-Einstein condensation.[8-9]

In this paper, we report on the Auger exciton-exciton annihilation process in layered BiI_3 using a luminescence technique. BiI_3 belongs to a family of layered metal halides which are composed of strongly bonded two-dimensional layers with weak van der Waals interlayer coupling. Below the fundamental indirect absorption edge, BiI_3 has stacking-fault excitons called R, S, and T. These excitons are not localized and are considered two-dimensional Frenkel excitons confined in the stacking-fault planes.[10-13] The exciton peaks show very sharp structures and are located very close to each other. The relaxation processes among these levels are of great interest in these special semiconductor materials. Thus the cascade relaxation process and the coherent phenomena of the stacking-fault excitons have been well studied.[14,15]

The sample used in this experiment was grown by the sublimation method, under the condition of excess iodine in the gas phase. For the luminescence measurement, the sample was directly immersed in liquid helium. The laser system comprised a cw mode-locked Nd^{3+}:YAG (yttrium aluminum garnet) laser, a fiber pulse compressor, a second-harmonic generator, and a cavity-dumped dye laser. The pulse width, the repetition rate, and the wavelength of the second harmonic of the fiber-compressed cw mode-locked Nd^{3+}:YAG laser are 6 ps, 82 MHz, and 532 nm, respectively. The cavity-dumped dye laser is synchronously pumped by the second harmonic and tuned to 584 nm. The repetition rate of the output of the dye laser can be changed and its pulse width is about 700 fs. The excitation efficiency at 532 nm is about six times larger than that at 584 nm, and no other essential difference is observed between the two excitation wavelengths. Thus both the second-harmonic output of 532 nm and the dye laser output of 584 nm were used as the excitation light source in the experiment.

The absorption spectrum and the luminescence spectrum of the R, S, and T excitons of BiI_3 at 4.2 K are shown in Figs. 1(a) and 1(b), respectively. Both the ab-

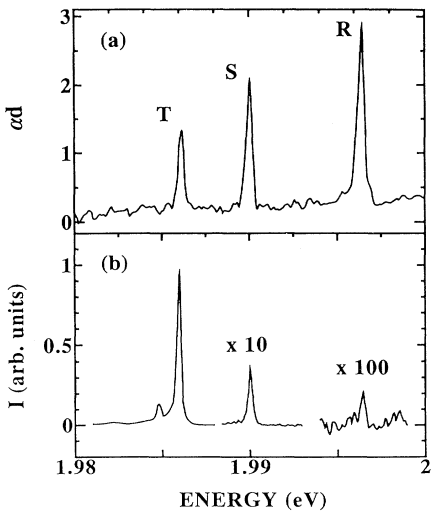

FIG. 1. The absorption (a) and luminescence (b) spectra of the stacking-fault excitons R, S, and T in BiI_3 layered crystals at 4.2 K. Three peaks are very sharp and there is no detectable energy shift between the absorption and luminescence peaks. Though three absorption peaks show similar peak intensities, the higher-energy exciton shows much weaker luminescence intensity.

sorption and luminescence spectra show three structures with full width at half maximum (FWHM) as sharp as 0.3 meV, and there is no detectable Stokes shift. This result indicates that the homogeneity of the stacking-fault planes is high and that the R, S, and T excitons form an ideal multilevel exciton system. The difference of the relative intensities between the absorption and luminescence peaks reveals the internal relaxation of the excitons, since the higher-energy exciton shows significantly weaker luminescence in spite of its stronger absorption.

Figure 2(a) is a schematic diagram of the cascade relaxation process among the R, S, and T exciton levels. The levels labeled G and B correspond to the ground state and the absorption band, respectively. The photoexcited carriers relax from higher levels to lower levels in turn. Figure 2(b) shows the typical time-resolved luminescence of the R, S, and T excitons observed by means of a streak camera. The excitation pulses were second harmonics of the pulse-compressed Nd^{3+}:YAG laser, and the excitation pulse energy density was 6.75 nJ/cm^2. A subtractive-dispersion double monochromator was used to compensate for the group-velocity dispersion in the monochromator. The laser pulse was also monitored simultaneously with the luminescence signal in order to know the time jitter during the signal accumulation. The total time resolution achieved in this configuration was 16 ps. The R, S, and T excitons show different relaxation rates, with the lower-energy exciton showing the slower decay. This behavior is similar to that reported by Akai *et al.*, and is explained by the cascade relaxation model.[14] In addition to the relaxation, the short time resolution of the streak camera enabled us to observe clearly the rises of the S and T excitons. The rises more clearly support the cascade relaxation model.

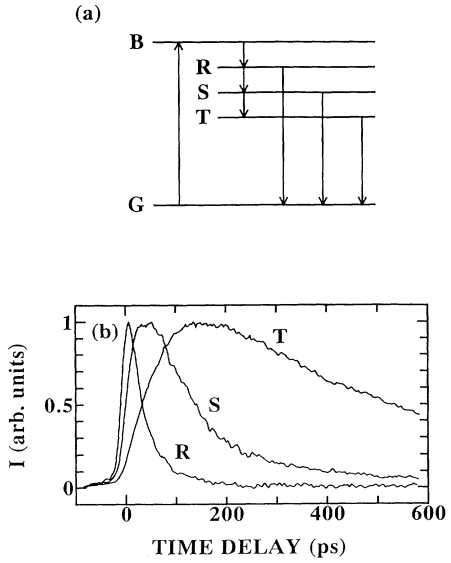

FIG. 2. (a) The cascade relaxation diagram of the stacking-fault excitons R, S, and T. The levels labeled G and B correspond to the ground state and the absorption band. (b) Typical time-resolved luminescence intensities of the R, S, and T excitons. The excitation energy density, the repetition rate, and the wavelength of the excitation pulses are 6.8 nJ/cm^2, 82 MHz, and 532 nm, respectively. The lower-energy exciton shows the slower rise and slower decay as a result of the cascade relaxation process.

The excitation density dependence of the intensity of the time-integrated luminescence of the stacking-fault excitons is displayed in Fig. 3. The excitation light source is the second harmonic of the Nd^{3+}:YAG laser. The circles, the squares, and the triangles correspond to the intensity of the T, S, and R excitons. The straight lines are used as guides for the eye. The intensities of the R, S, and T excitons saturate at the different excitation levels, as indicated by the arrows. The lower-energy exciton saturates at the lower excitation density. The luminescence efficiencies of the R, S, and T excitons all decrease with an increase in the excitation density. Thus phase-space filling in the cascade relaxation process cannot explain the experimental result, since the saturation of a lower level should result in an increase in the occupation of the higher levels, which should give rise to greater luminescence from these higher levels. This is not observed, and so phase-space filling does not explain our observations.

Figure 4(a) shows the temporal changes of the T exciton luminescence at the excitation densities of 0.92 and 66 nJ/cm^2. The excitation light source is the second harmonic of the Nd^{3+}:YAG laser. The relaxation rate increases as the excitation density is raised. Moreover, the signal at the high excitation density shows a clear nonexponential decay, though the signal at the low excitation density shows an exponential decay. It is reasonable to assume that the luminescence intensity is proportional to the exciton density. Thus the decrease in the luminescence efficiency and the appearance of the rapid decay indicate a branching of the excitons into a nonradiative path. We introduce the Auger exciton-exciton annihilation process to explain this high-density carrier effect. The following is the rate equation for the T exciton including the exciton-exciton annihilation process,

$$\frac{dn}{dt} = -\gamma n - \beta n^2 + f(t) , \tag{1}$$

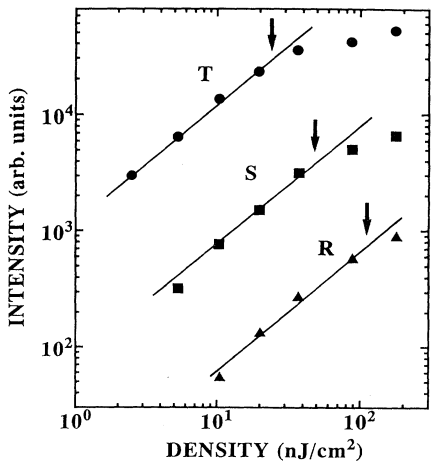

FIG. 3. The excitation energy density dependence of the time-integrated luminescence intensities of the R, S, and T excitons. As indicated by arrows, the saturation occurs at the different excitation levels for the R, S, and T excitons.

where n is the density of the T exciton, γ and β are the linear decay rate and the annihilation rate caused by exciton-exciton collisions, respectively, and $f(t)$ is the source term which is mainly attributable to the population of the S exciton. The dots plotted in Fig. 4(a) are the fits from Eq. (1). The T exciton density n is normalized by the peak value of the luminescence data at the excitation density 66.1 nJ/cm^2. We fit these decay curves using two parameters of $\gamma=1.5$ ns^{-1} and $\beta=4.53$ ns^{-1}, respectively. The data before 250 ps are excluded from the fitting procedure and the source term $f(t)$ is taken to be 0, since the S exciton is negligible after 250 ps, as shown by the dotted line in Fig. 4(a). Figure 4(b) shows the time-resolved luminescence of the S exciton at the excitation densities of 2.3 and 66 nJ/cm^2. The temporal change of the S exciton depends on the excitation density in a similar way to that of the T exciton. However, we cannot obtain reliable fitting parameters for the S exciton, because the excitation density dependence is not prominent enough to give the nonlinear parameter β, and because the Auger process between the S and T excitons complicates the analysis.

In order to verify the high-density effect of the stacking-fault excitons more clearly, we measured the time-resolved nonlinear luminescence signal, since time-resolved nonlinear luminescence techniques directly provide information about nonlinear carrier dynamics. Time-resolved nonlinear luminescence spectroscopy has been successfully applied to the measurement of the recombination rate of excitons in CdSe and GaAs quantum wells.[16,17] The following is the experimental procedure for time-resolved nonlinear luminescence. The laser beam is divided into two beams by a beam splitter, and they are crossed at the sample. The timing τ between the pulses of the two beams is adjusted by an optical time delay. The two beams are chopped at two different frequencies, Ω_1 and Ω_2, respectively. The $\Omega_1+\Omega_2$ component of the luminescence signal is detected by a lock-in technique in order to select the nonlinear component of the luminescence. The experimental results of the nonlinear luminescence of T and S excitons are displayed in Figs. 5(a) and 5(b), respectively.

In the actual experiment, the nonlinear luminescence signal is also sensitive to the thermal effect. If excitation pulses of a high repetition rate are used, the nonlinear luminescence spectrum shows a dispersive form reflecting the thermal spectral shift, and a constant base appears in the time trace signal. To eliminate this thermal effect from the nonlinear luminescence signal, we used the cavity-dumped dye laser output and reduced the repetition rate of the laser pulses.

The dots plotted in Fig. 5(a) are the experimental result of the time correlation of the nonlinear T exciton

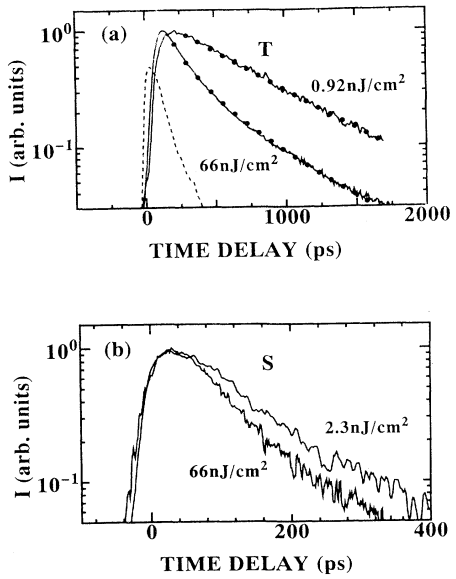

FIG. 4. The excitation density dependence of the time-resolved luminescence of the stacking-fault excitons. (a) The solid lines are the experimental data of the T exciton. The decay rate increases as the excitation density is raised. The dots are the theoretical fit obtained by using Eq. (1). The density of the T exciton is normalized to the peak value for that at 66.1 nJ/cm^2. The fitting parameters γ and β are 1.5 and 4.53 ns^{-1}, respectively. We exclude the data before 250 ps from the fittings for simplicity so as to avoid the contribution from the S and R excitons. After 250 ps, the densities of S and R excitons are low enough that the source term $f(t)$ can be taken to be 0. The broken line is the signal of the S exciton for comparison. (b) Data for the S exciton. The excitation density dependence of the S exciton is similar to that of the T exciton.

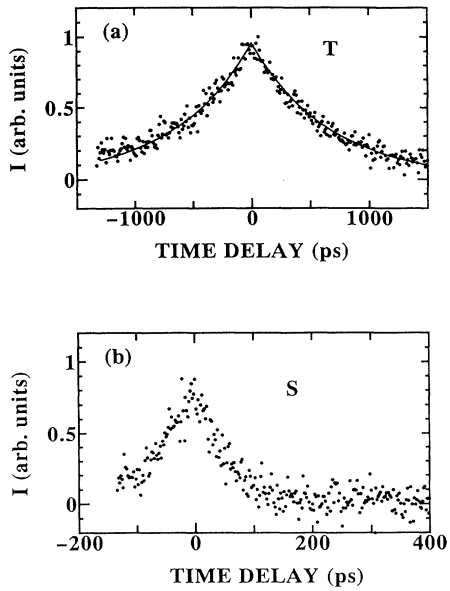

FIG. 5. The time-resolved nonlinear luminescence correlations of the stacking-fault excitons. The wavelength and the repetition rate of the laser pulses are 584 nm and 4.1 MHz, respectively. The excitation energy densities of the two beams are the same. (a) The signal of the T exciton at the excitation density 43.3 nJ/cm^2. The dots are the experimental data and the solid line is the theoretical curve based on the Auger exciton-exciton annihilation process. The same parameters that are used for Fig. 4(a) are used. (b) The signal of the R exciton at the energy density 88.0 nJ/cm^2. The signal gives roughly the lifetime of the R exciton, and the origin is the same as that of the T exciton.

luminescence. We have calculated the nonlinear luminescence signal of the T exciton as follows. Equation (1) is integrated, and the temporal change of the time-integrated intensity is calculated as a function of the decay time τ. Here we used the relation

$$f(t)=n_0[\delta(t)+\delta(t-\tau)] , \quad (2)$$

where n_0 is the initial density of T excitons injected by the first and the second excitation pulses, and τ is the interval between two pulses. Taking into account the smaller quantum yield of the 583-nm excitation, the value n_0 is taken to be 0.11. In this calculation, we have neglected the finite lifetime of the S exciton and used the δ function in the source term. The lifetime of the R exciton is shorter than that of the T exciton and does not affect the result significantly. The solid line shown in Fig. 5(a) is the fit using the same parameters as for the fit of Fig. 4(a). The nonlinear luminescence signal of the S exciton is also displayed in Fig. 5(b). We do not fit the experimental data because we could not obtain the nonlinear parameter β, as discussed above. The data roughly reflect the lifetime of the S exciton.

The prominent Auger process of the stacking-fault excitons may be attributable to the large density of the final state. The initial state of the Auger process is the surface state of the stacking disorder. The final state, which results from the annihilation of an exciton-exciton pair, consists of a free electron and a free hole whose energies lie deep in the band states of bulk crystal. Thus the final-state density is much larger than the initial state. Once the high-energy free carriers are generated in the bulk, they easily branch into nonradiative paths. This efficient branching into nonradiative paths explains the clear nonexponential decay of the T exciton. The indirect nature of the fundamental absorption edge of BiI_3 (Ref. 13) may also contribute to the nonradiative process. However, the electronic structure of BiI_3 is also responsible for the process, and we cannot refer to this point further. In order to clarify the high-density excitation effect, further experimental and the theoretical studies are needed.

In conclusion, we have studied the optical nonlinearity of the stacking-fault excitons of BiI_3 by way of luminescence measurements. In addition to the decay rates of the R, S, and T excitons, the 16-ps time resolution of the streak camera reveals a clear rise in luminescence of the T and S excitons, which is direct evidence of the cascade relaxation process among the stacking-fault excitons. As the excitation density is raised, a decrease in luminescence efficiency and an increase in the decay rate are observed. At the high excitation density, we observed an obvious nonexponential decay of the T exciton, which is attributable to the Auger exciton-exciton annihilation process. The nonexponential decay is well fitted by a rate equation with an exciton-exciton annihilation term. The time-correlation technique of the nonlinear luminescence also gives a result consistent with the nonexponential decay of the T exciton. The experimental results give us a unique example of a prominent Auger process and nonlinearity of multilevel excitons in semiconductors.

This work was supported by Scientific Research Grants-in-Aid Nos. 03740157 and 03402007 from the Ministry of Education, Science and Culture of Japan.

*Present address: Opto-Electronics Research Laboratories, NEC Corporation, Tsukuba, Ibaraki 305, Japan.

[1]H. Lobentanzer, W. W. Rühle, H.-J. Polland, W. Stolz, and K. Ploog, Phys. Rev. B **36**, 2954 (1987).
[2]T. C. Damen, Karl Leo, Jagdeep Shah, and J. E. Cunningham, Appl. Phys. Lett. **58**, 1902 (1991).
[3]D. W. Snoke, W. W. Rühle, Y.-C. Lu, and E. Bauser, Phys. Rev. Lett. **68**, 990 (1992).
[4]X. Q. Zhou, K. Leo, and H. Kurz, Phys. Rev. B **45**, 3886 (1992).
[5]Y. Rosenwaks, Y. Shapira, and D. Huppert, Phys. Rev. B **45**, 9108 (1992).
[6]G. C. Osbourn and D. L. Smith, Phys. Rev. B **20**, 1556 (1979).
[7]Shui Lai and M. V. Klein, Phys. Rev. B **29**, 3217 (1984).
[8]A. Mysyrowicz, D. Hulin, and C. Benoit à la Guillaume, J. Lumin. **24/25**, 629 (1981).
[9]D. W. Snoke and J. P. Wolfe, Phys. Rev. B **42**, 7876 (1990).
[10]E. F. Gross, V. I. Perel, and R. I. Shekhmamet'ev, Pis'ma Zh. Eksp. Teor. Fiz. **13**, 320 (1971) [JETP Lett. **13**, 229 (1971)].
[11]Y. Kaifu and T. Komatsu, J. Phys. Soc. Jpn. **40**, 1377 (1976).
[12]K. Watanabe, T. Karasawa, T. Komatsu, and Y. Kaifu, J. Phys. Soc. Jpn. **55**, 897 (1986).
[13]Y. Kaifu, J. Lumin. **42**, 61 (1988).
[14]I. Akai, T. Karasawa, Y. Kaifu, A. Nakamura, M. Shimura, and M. Hirai, J. Lumin. **42**, 357 (1989).
[15]T. Karasawa, M. Ichida, I. Akai, and T. Komatsu, Appl. Phys. A **53**, 480 (1991).
[16]M. Jørgensen and J. M. Hvam, Appl. Phys. Lett. **43**, 460 (1983).
[17]S. Ideshita and Y. Masumoto, J. Phys. Soc. Jpn. **59**, 331 (1990).